Inorg. Chem. **2009**, *48*, 2605−2613

Self-Assembled Pd(II) Metallocycles Using an Ambidentate Donor and the Study of Square−Triangle Equilibria

Sushobhan Ghosh and Partha Sarathi Mukherjee*

Department of Inorganic and Physical Chemistry, Indian Institute of Science, Bangalore-560 012, India

Received November 24, 2008

The self-assembly reaction of a *cis*-blocked 90° square planar metal acceptor with a symmetrical linear flexible linker is expected to yield a [4 + 4] self-assembled square, a [3 + 3] assembled triangle, or a mixture of these. However, if the ligand is a nonsymmetrical ambidentate, it is expected to form a complex mixture comprising several linkage isomeric squares and triangles as a result of different connectivities of the ambidentate linker. We report instead that the reaction of a 90° acceptor *cis*-(dppf)Pd(OTf)$_2$ [where dppf = 1,1′-bis(diphenylphosphino)-ferrocene] with an equimolar amount of the ambidentate unsymmetrical ligand Na-isonicotinate unexpectedly yields a mixture of symmetrical triangles and squares in the solution. An analogous reaction using *cis*-(tmen)Pd(NO$_3$)$_2$ instead of *cis*-(dppf)Pd(OTf)$_2$ also produced a mixture of symmetrical triangles and squares in the solution. In both cases the square was isolated as the sole product in the solid state, which was characterized by a single crystal structure analysis. The equilibrium between the triangle and the square in the solution is governed by the enthalpic and entropic contributions. The former parameter favors the formation of the square due to less strain in the structure whereas the latter one favors the formation of triangles due to the formation of more triangles from the same number of starting linkers. The effects of temperature and concentration on the equilibria have been studied by NMR techniques. This represents the first report on the study of square-triangle equilibria obtained using a nonsymmetric ambidentate linker. Detail NMR spectroscopy along with the ESI−mass spectrometry unambiguously identified the components in the mixture while the X-ray structure analysis determined the solid-state structure.

Introduction

The design and synthesis of discrete molecular architectures via directional self-assembly of polytopic organic donors and metal based acceptors have undergone significant development for more than a decade.[1] There are many examples of molecular architectures prepared using a directional self-assembly approach including rhomboids, triangles, squares, rectangles, pentagons, hexagons, and many other structures of complex topologies.[2−8] The simplest reaction among all the known directional self-assembly reactions is the assembly of a 90° ditopic acceptor with one equivalent linear donor. The expected product for this combination should be a [4 + 4] self-assembled molecular square. In fact, Fujita et al. reported in 1990 the exclusive formation of a molecular square using this approach from the combination of *cis*-(en)Pd(NO$_3$)$_2$ and 4,4′-bipyridine.[9,10] Later on, was established that the combination of a *cis*-blocked square planar metal acceptor with a linear donor can yield, in some

* To whom correspondence should be addressed. E-mail: psm@ipc.iisc.ernet.in. Fax: 91-80-2360-1552. Tel: 91-80-2293-3352.

(1) (a) Lehn, J.-M. *Supramolecular Chemistry, concepts and perspectives*; VCH: New York, 1995. (b) Seidel, S. R.; Stang, P. J. *Acc. Chem. Res.* **2002**, *35*, 972. (c) Leininger, S.; Olenyuk, B.; Stang, P. J. *Chem. Rev.* **2000**, *100*, 853. (d) Cotton, F. A.; Lin, C.; Murillo, C. A. *Acc. Chem. Res.* **2001**, *34*, 759. (e) Maurizot, V.; Yoshizawa, M.; Kawano, M.; Fujita, M. *Dalton Trans.* **2006**, 2750. (f) Nehete, U. N.; Anantharaman, G.; Chandrasekhar, V.; Murugavel, R.; Roesky, H. W.; Vidovic, D.; Magull, J.; Samwer, K.; Sass, B. J. *Angew. Chem., Int. Ed.* **2004**, *43*, 3832. (g) Ghosh, A. K.; Ghoshal, D.; Ribas, J.; Mostafa, G.; Chaudhuri, N. R. *Cryst. Growth Des.* **2006**, *6*, 36. (h) Campos-Fernandez, C. S.; Schottel, B. L.; Chifotides, H. T.; Bera, J. K.; Bacsa, J.; Koomen, J. M.; Russell, D. H.; Dunbar, K. R. *J. Am. Chem. Soc.* **2005**, *127*, 12909. (i) Schalley, C. A.; Lutzen, A.; Albrecht, M. *Chem. -Eur. J.* **2004**, *10*, 1072. (j) Northrop, B. J.; Yang, H.-B.; Stang, P. J. *Chem. Commun.* **2008**, 5896. (k) Zangrando, E.; Casanova, M.; Alessio, E. *Chem. Rev.* **2008**, *108*, 4979.

(2) (a) Yamamoto, T.; Arif, A. M.; Stang, P. J. *J. Am. Chem. Soc.* **2003**, *125*, 12309. (b) Ghosh, S.; Chakrabarty, R.; Mukherjee, P. S. *Dalton Trans.* **2008**, 1850. (c) Horikoshi, R.; Mikuriya, M. *Cryst. Growth Des.* **2005**, *5*, 223. (d) Slone, R. V.; Benkstein, K. D.; Bélanger, S.; Hupp, J. T.; Guzei, I. A.; Rheingold, A. L. *Coord. Chem. Rev.* **1998**, *171*, 221. (e) Dash, B. P.; Satapathy, R.; Maguire, J. A.; Hosmane, N. S. *Org. Lett.* **2008**, *10*, 2247. (f) Nehete, U. N.; Anantharaman, G.; Chandrasekhar, V.; Murugavel, R.; Roesky, H. W.; Vidovic, D.; Magull, J.; Samwer, K.; Sass, B. J. *Angew. Chem., Int. Ed.* **2004**, *43*, 3832.

10.1021/ic802254f CCC: $40.75
Published on Web 02/19/2009

cases, interesting equilibrium between a molecular triangle and the expected square. Further research established that the relative amount of the components (square or triangle) depends upon concentration of the components, temperature of the reaction medium, and amount of the reacting components.[11] The driving force for such self-assembly reaction is under thermodynamic control. The molecular square is wider and less strained compared to the triangle, and thus enthalpy favors the formation of the square. On the other hand, entropy favors the formation of a triangle since more triangles compared to squares are formed from the same number of starting building units. As a result of this thermodynamic balance, triangles become the major products in equilibrium if the ligands are flexible and reduce the strain by allowing the ligand to bend. Similarly, the squares become the major entity of the mixture if the reacting ligands are too rigid so that the enthalpic benefit overcomes the entropic penalty in the square formation.[12,13] In a majority of the cases, for the design of discrete molecular architectures, symmetrical polypyridyl ligands have been used with a few recent examples where we and others have utilized symmetrical oxygen donor ligands with Pt(II) acceptors to generate neutral assemblies.[5a,13d,14] Nonsymmetric/ambidentate bridging ligands are not the right choices for this purpose since they may generate a mixture of isomers due to different connectivities, and thus it is difficult to control both the reaction and the isolation of the products in pure form.[14a,b] Despite the possibility of formation of several linkage isomers, our recent report established the selective formation of a single isomeric triangle using a nonsymmetric ambidentate nicotinate donor and a Pd(II) 90° acceptor.[14a] To the best of our knowledge the formation of a triangle−square equilibrium using a nonsymmetrical ambidentate ligand has not so far been reported. The present paper reports the synthesis and characterization of two self-assembled macrocyclic squares (**1a**, **2a**) from *cis*-(LL)Pd(X)$_2$ and nonsymmetric isonicotinate donor [where LL = 1,1′-bis(diphenylphosphino)ferrocene (dppf), X = $CF_3SO_3^-$ for **1a** and LL = *N*,*N*,*N*′,*N*′-tetramethylethane-1,2-diamine (tmen), X =

(3) (a) Derossi, S.; Casanova, M.; Lengo, E.; Zangrando, E.; Stener, M.; Alessio, E. *Inorg. Chem.* **2007**, *46*, 11243. (b) Ghosh, S.; Turner, D. R.; Batten, S. R.; Mukherjee, P. S. *Dalton Trans.* **2007**, 1869. (c) Fujita, M.; Aoyagi, M.; Ogura, K. *Inorg. Chim. Acta* **1996**, *246*, 53. (d) Schnebeck, R.-D.; Randaccio, L.; Zangrando, E.; Lippert, B. *Angew. Chem., Int. Ed.* **1998**, *37*, 119. (e) Lai, S.-W.; Chan, M. C.-W.; Peng, S.-M.; Che, C.-M. *Angew. Chem., Int. Ed.* **1999**, *38*, 669. (f) Habereder, T.; Warchhold, M.; Noth, H.; Severin, K. *Angew. Chem., Int. Ed.* **1999**, *38*, 3225. (g) Sun, S.-S.; Lees, A. J. *Inorg. Chem.* **1999**, *38*, 4181. (h) Schneebeck, R.-D.; Friesinger, E.; Glahe, F.; Lippert, B. *J. Am. Chem. Soc.* **2000**, *122*, 1381–1390. (i) Yu, X.-Y.; Maekawa, M.; Kondo, M.; Kitagawa, S.; Jin, G.-X. *Chem. Lett.* **2001**, 168. (j) Schweiger, M.; Seidel, S. R.; Arif, A. M.; Stang, P. J. *Angew. Chem., Int. Ed.* **2001**, *40*, 3467. (k) Lee, S. J.; Hu, A.; Lin, W. *J. Am. Chem. Soc.* **2002**, *124*, 12948. (l) Fornies, J.; Gomez, J.; Lalinde, E.; Moreno, M. T. *Chem. Eur. J.* **2004**, *10*, 888. (m) Drain, C. M.; Lehn, J. M. *Chem. Commun.* **1994**, 2313. (n) Manna, J.; Whiteford, J. A.; Stang, P. J.; Muddiman, D. C.; Smith, R. D. *J. Am. Chem. Soc.* **1996**, *118*, 8731.

(4) (a) Wurthner, F.; You, C.-C.; Saha-Moller, C. R. *Chem. Soc. Rev.* **2004**, *33*, 133. (b) Fujita, M.; Sasaki, O.; Mitsuhashi, T.; Fujita, T.; Yazaki, J.; Yamaguchi, K.; Ogura, K. *Chem. Commun.* **1996**, 1535. (c) Whiteford, J. A.; Stang, P. J.; Huang, D. S. *Inorg. Chem.* **1998**, *37*, 5595. (d) Manna, J.; Kuehl, C. J.; Whiteford, J. A.; Stang, P. J.; Muddiman, D. C.; Hofstadler, S. A.; Smith, R. D. *J. Am. Chem. Soc.* **1997**, *119*, 11611. (e) Olenyuk, B.; Whiteford, J. A.; Stang, P. J. *J. Am. Chem. Soc.* **1996**, *118*, 8221. (f) Stang, P. J.; Olenyuk, B. *Angew. Chem., Int. Ed.* **1996**, *35*, 732. (g) Kraft, S.; Hanuschek, E.; Beckhaus, R.; Haase, D.; Saak, W. *Chem. Eur. J.* **2005**, *11*, 969. (h) He, Z.; He, C.; Wang, Z.-M.; Gao, E.-Q.; Liu, Y.; Yan, C.-H. *Dalton Trans.* **2004**, 502.

(5) (a) Mukherjee, P. S.; Das, N.; Kryschenko, Y. K.; Arif, M. A.; Stang, P. J. *J. Am. Chem. Soc.* **2004**, *126*, 2464. (b) Kuehl, C. J.; Huang, S. D.; Songping, D.; Stang, P. J. *J. Am. Chem. Soc.* **2001**, *123*, 9634. (c) Ghosh, S.; Mukherjee, P. S. *Dalton Trans.* **2007**, 2542. (d) Wu, J.-Y.; Thanasekaran, P.; Cheng, Y.-W.; Lee, C.-C.; Manimaran, B.; Rajendran, T.; Liao, R.-T.; Lee, G.-H.; Peng, S.-M.; Lu, K.-L. *Organometallics* **2008**, *27*, 2141. (e) Northrop, B. H.; Glockner, A.; Stang, P. J. *J. Org. Chem.* **2008**, *73*, 1787. (f) Gomez, L.; Company, A.; Fontrodona, X.; Ribas, X.; Costas, M. *Chem. Commun.* **2007**, 4410. (g) Li, S.-S.; Yan, H.-J.; Wan, L.-J.; Yang, H.-B.; Northrop, B. H.; Stang, P. J. *J. Am. Chem. Soc.* **2007**, *129*, 9268. (h) Kim, D.; Paek, J. H.; Jun, M.-J.; Lee, J. Y.; Kang, S. O.; Ko, J. *Inorg. Chem.* **2005**, *44*, 7886. (i) Crowley, J. D.; Bosnich, B. *Eur. J. Inorg. Chem.* **2005**, 2015. (j) Das, N.; Arif, A. M.; Stang, P. J. *Inorg. Chem.* **2005**, *44*, 5798. (k) Thanasekaran, P.; Liao, R. T.; Liu, Y.-H.; Rajendran, T.; Rajagopal, S.; Lu, K.-L. *Coord. Chem. Rev.* **2005**, *249*, 1085. (l) Manimaran, B.; Thanasekaran, P.; Rajendran, T.; Lin, R.-J.; Chang, I.-J.; Lee, G.-H.; Peng, S.-M.; Rajagopal, S.; Lu, K.-L. *Inorg. Chem.* **2002**, *41*, 5323.

(6) (a) Blum, M.-C.; Cavar, E.; Pivetta, M.; Patthey, F.; Schneider, W.-D. *Angew. Chem., Int. Ed.* **2005**, *44*, 5334. (b) Pivetta, M.; Blum, M.-C.; Patthey, F.; Schneider, W.-D. *Angew. Chem., Int. Ed.* **2008**, *47*, 1076. Olson, A. J.; Hu, Y. H. E.; Keinan, E. *Proc. Natl. Acad. Sci. U.S.A.* **2007**, *104*, 20731.

(7) (a) Yang, H.-B.; Das, N.; Huang, F.; Hawkridge, A. M.; Muddiman, D. C.; Stang, P. J. *J. Am. Chem. Soc.* **2006**, *128*, 10014. (b) Stang, P. J.; Persky, N. E.; Manna, J. *J. Am. Chem. Soc.* **1997**, *119*, 4777. (c) Hasegawa, M.; Enozawa, H.; Kawabata, Y.; Iyoda, M. *J. Am. Chem. Soc.* **2007**, *129*, 3072.

(8) (a) Olenyuk, B.; Whiteford, J. A.; Fechtenkotter, A.; Stang, P. J. *Nature* **1999**, *398*, 796. (b) Ghosh, S.; Chakrabarty, R.; Mukherjee, P. S. *Inorg. Chem.* **2009**, *48*, 549. (c) Takeda, N.; Umemoto, K.; Yamaguchi, K.; Fujita, M. *Nature* **1999**, *398*, 794. (d) Ghosh, S.; Mukherjee, P. S. *J. Org. Chem.* **2006**, *71*, 8412. (e) Kamiya, N.; Tominaga, M.; Sato, S.; Fujita, M. *J. Am. Chem. Soc.* **2007**, *129*, 3816. (f) Suzuki, K.; Kawano, M.; Sato, S.; Fujita, M. *J. Am. Chem. Soc.* **2007**, *129*, 10652. (g) Wang, Y.; Quillian, B.; Wei, P.; Wannere, C. S.; Schleyer, P. V. R.; Robinson, G. H. *Organometallics* **2006**, *25*, 3286. (h) Saha, S.; Johansson, E.; Flood, A. H.; Tseng, H. R.; Zink, J. I.; Stoddart, J. F. *Chem. Eur. J.* **2005**, *11*, 6846. (i) Westcott, A.; Fisher, J.; Harding, L. P.; Rizkallah, P.; Hardie, M. J. *J. Am. Chem. Soc.* **2008**, *130*, 2950. (j) Yang, H.-B.; Ghosh, K.; Arif, A. M.; Stang, P. J. *J. Org. Chem.* **2006**, *71*, 9464. (k) Garrison, J. C.; Panzner, M. J.; Custer, P. D.; Reddy, D. V.; Rinaldi, P. L.; Tessier, C. A.; Youngs, W. J. *Chem. Commun.* **2006**, 4644. (l) Muller, I. M.; Moller, D. *Angew. Chem., Int. Ed.* **2005**, *44*, 2969. (m) Süss-Fink, G.; Therrien, B. *Organometallics* **2007**, *26*, 766. (n) Govindaswamy, P.; Therrien, B.; Süss-Fink, G. *Organometallics* **2007**, *26*, 915. (o) Therrien, B.; Süss-Fink, G.; Govindaswamy, P.; Renfrew, A. K.; Dyson, P. D. *Angew. Chem., Int. Ed.* **2008**, *47*, 3773.

(9) Fujita, M.; Yazaki, J.; Ogura, K. *J. Am. Chem. Soc.* **1990**, *112*, 5645.

(10) (a) Zahng, L.; Niu, Y.-H.; Jen, A. K.-Y.; Lin, W. *Chem. Commun.* **2005**, 1002. (b) Kieltyka, R.; Englebienne, P.; Fakhoury, J.; Autexier, C.; Moitessier, N.; Sleiman, H. F. *J. Am. Chem. Soc.* **2008**, *130*, 10040.

(11) (a) Ferrer, M.; Mounir, M.; Rossell, O.; Ruiz, E.; Maestro, M. A. *Inorg. Chem.* **2003**, *42*, 5890. (b) Schweiger, M.; Seidel, S. R.; Arif, A. M.; Stang, P. J. *Inorg. Chem.* **2002**, *41*, 2556. (c) Weilandt, T.; Troff, R. W.; Saxell, H.; Rissanen, K.; Schalley, C. A. *Inorg. Chem.* **2008**, *47*, 7588.

(12) Lee, S. B.; Hwang, S.; Chung, D. S.; Yun, H.; Hong, J.-I. *Tetrahedron Lett.* **1998**, *39*, 873.

(13) (a) Cotton, F. A.; Daniels, L. M.; Lin, C.; Murillo, C. A. *J. Am. Chem. Soc.* **1999**, *121*, 4538. (b) Fujita, M.; Aoyagi, M.; Ogura, K. *Inorg. Chem. Acta.* **1996**, *246*, 53. (c) Mukherjee, P. S.; Ghosal, D.; Zangrando, E.; Mallah, T.; Chaudhuri, N. R. *Eur. J. Inorg. Chem.* **2004**, 4675. (d) Sun, S.-S.; Lees, A. J. *J. Am. Chem. Soc.* **2000**, *122*, 8956. (e) Das, N.; Mukerjee, P. S.; Arif, A. M.; Stang, P. J. *J. Am. Chem. Soc.* **2003**, *125*, 13950.

(14) (a) Ghosh, S.; Batten, S. R.; Turner, D.; Mukherjee, P. S. *Dalton Trans.* **2007**, 1869. (b) Ghosh, S.; Mukherjee, P. S. *Dalton Trans.* **2007**, 2542. (c) Teo, P.; Koh, L. L.; Hor, T. S. A. *Chem. Commun.* **2007**, 4221. (d) Teo, P.; Koh, L. L.; Hor, T. S. A. *Chem. Commun.* **2007**, 2225. (e) Chi, K.-W.; Addicott, C.; Arif, A. M.; Stang, P. J. *J. Am. Chem. Soc.* **2004**, *126*, 16569. (f) Chi, K-.W.; Addicott, C.; Moon, M.-E.; Lee, H. J.; Yoon, S. C.; Stang, P. J. *J. Org. Chem.* **2006**, *71*, 6662. (g) Teo, P.; Koh, L. L.; Hor, T. S. A. *Inorg. Chem.* **2003**, *42*, 7290.

Scheme 1. Self-Assembly of Inter-Converting Molecular Squares and Triangles from an Ambidentate Linker Isonicotinate and *cis*-Protected 90° Palladium Acceptors

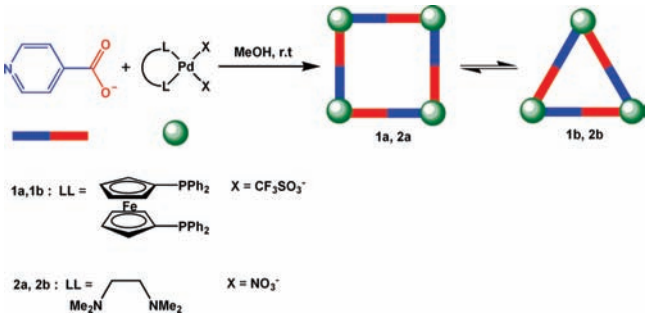

NO_3^- for **2a**] (Scheme 1). The ligand isonicotinate was considered to be flexible because of the presence of the carboxyl group, and the electron on the donor sp^3 hybridized oxygen is not restricted in its orientation unlike that on the sp^2 hybridized pyridyl nitrogen. The formation of triangle−square equilibria was established in both cases, and the equilibria between **1a**, **2a** (square) and **1b**, **2b** (triangle) and the relative amount of the components in the mixture were studied by electrospray ionization (ESI) mass spectrometry, diffusion ordered spectroscopy (DOSY) NMR, and variable temperature multinuclear NMR.

Result and Discussion

Synthesis and Characterization of the Metallamacrocycles. The primary target of this work was the synthesis of a molecular square using an ambidentate isonicotinate as a linear linker in combination with appropriate *cis*-blocked 90° Pd(II) acceptors. The preparation of the corner units *cis*-(dppf)Pd$(CF_3SO_3)_2$ and *cis*-(tmen)Pd$(NO_3)_2$ [tmen = *N*,*N*,*N*′,*N*′-tetramethylethane-1,2-diamine] involves the reaction of the corresponding dichloride with 2 equiv of AgOTf or $AgNO_3$, respectively, at ambient temperature. The self-assembly reactions were monitored by ^{1}H and ^{31}P NMR spectroscopy in solution. The *cis*-(dppf)Pd$(OTf)_2$ was treated with 1 equiv of sodium isonicotinate in methanol-d_4 for 1 h with continuous stirring to obtain a wine red solution. ^{31}P NMR (Figure 1) of the resulting solution showed the appearance of two major peaks at 38.8 ppm and 33.9 ppm of equal intensity with the complete disappearance of the peak at 46.4 ppm due to the starting *cis*-(dppf)Pd$(OTf)_2$. This upfield shift of the ^{31}P peak and the complete disappearance of the peak due to the starting linker indicated the ligand to metal coordination.[15]

Along with those major peaks are two small peaks at 38.7 and 35.3 ppm that appeared in the ^{31}P NMR spectrum. As a result of the nonsymmetrical nature of the donor linker, several linkage isomeric squares or triangles are expected for this combination (Figure 2). In case of symmetric isomers **1a** or **1b** two peaks in ^{31}P NMR with equal intensity are expected. For other expected nonsymmetrical linkage isomers (both for triangle and square) more than two peaks in ^{31}P NMR with appropriate intensity ratios are expected (Figure 2).

The smaller peaks are of equal intensity as well, and the relative intensity of the major and minor peaks does not fit

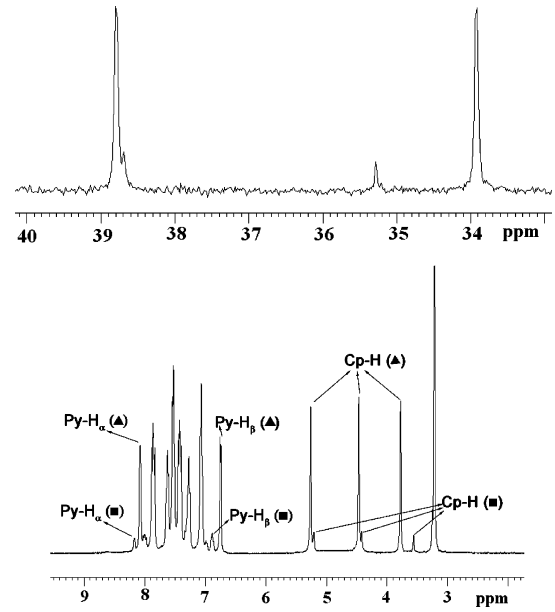

Figure 1. ^{31}P NMR (above) and ^{1}H NMR (below) spectra of **1a**−**1b** at 273 K.

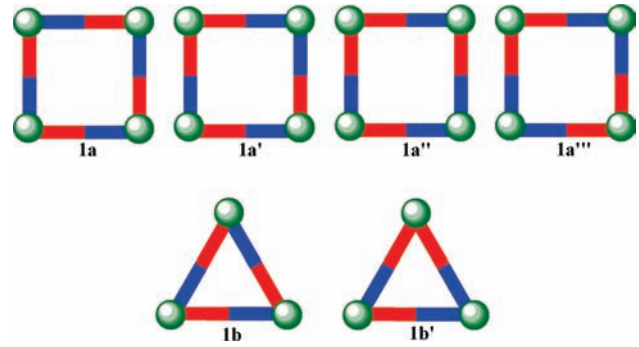

Figure 2. A few possible linkage isomers of squares and triangles.

with any expected nonsymmetrical square or triangle. This observation clearly suggests the formation of a mixture of two symmetrical macrocycles rather than the formation of nonsymmetrical analogues. Hence, a ^{31}P NMR study indicates the existence of both symmetrical square **1a** and triangle **1b** in solution. Proton NMR also (Figure 1) shows two sets of peaks for pyridine-H_α at 8.2 ppm (small) and 8.1 ppm (major) along with pyridine-H_β and cyclopentadienyl ring protons. The phenyl ring protons appeared as a multiplet in the region 7.1−7.9 ppm. The equimolar reaction between *cis*-(tmen)Pd$(NO_3)_2$ and sodium isonicotinate in methanol-d_4 was similarly monitored by ^{1}H NMR. The aromatic region

(15) (a) Jude, H.; Disteldorf, H.; Fischer, S.; Wedge, T.; Hawkridge, A. M.; Arif, A. M.; Hawthorne, M. F.; Muddiman, D. C.; Stang, P. J. *J. Am. Chem. Soc.* **2005**, *127*, 12131. (b) Jude, H.; Sinclair, D. J.; Das, N.; Sherburn, M. S.; Stang, P. J. *J. Org. Chem.* **2006**, *71*, 4155. (c) Schalley, C. A.; Muller, T.; Linnartz, P.; Witt, M.; Schafar, M.; Lutzen, A. *Chem. Eur. J.* **2002**, *8*, 3538. (d) Jeong, K. S.; Kim, S. Y.; Shin, U. S.; Kogej, M.; Hai, N. T. M.; Broekmann, P.; Jeong, N.; Kirchner, B.; Reither, M.; Schalley, C. A. *J. Am. Chem. Soc.* **2005**, *12*, 17672. (e) Mukherjee, P. S.; Das, N.; Stang, P. J. *J. Org. Chem.* **2004**, *69*, 3526. (f) Schweiger, M.; Seidel, S. R.; Schmitz, M.; Stang, P. J. *Org. Lett.* **2000**, *2*, 1255. (g) Fujita, M.; Yu, S. Y.; Kusukawa, T.; Funaki, H.; Ogura, K.; Yamaguchi, K. *Angew. Chem., Int. Ed.* **1998**, *37*, 2082. (h) Mukherjee, P. S.; Min, K. S.; Arif, A. M.; Stang, P. S. *Inorg. Chem.* **2004**, *43*, 6345. (i) Fujita, M.; Sasaki, O.; Mitsuhashi, T.; Fujita, T.; Yazaki, J.; Yamaguchi, K.; Ogura, K. *Chem. Commun.* **1996**, 1535.

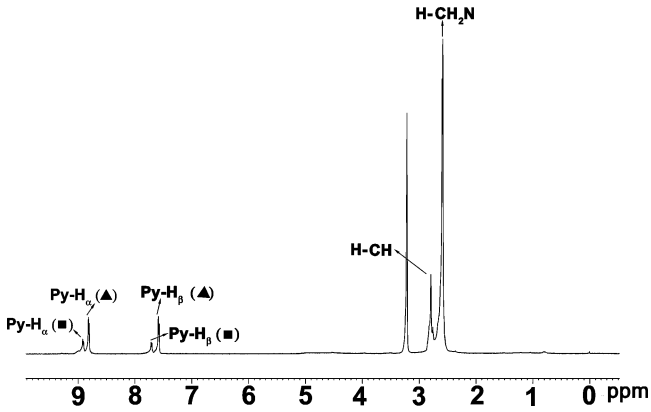

Figure 3. ^{1}H NMR spectra for **2a**−**2b** at 293 K.

of the ^{1}H NMR spectra showed the appearance of two peaks at 8.8 ppm and 7.6 ppm along with two more peaks of low intensity at 8.9 and 7.7 ppm (Figure 3).

The peaks at 8.8 and 8.9 ppm are 0.3 and 0.4 ppm downfield shifted, respectively, with respect to the H_α of isonicotinate whereas the peaks at 7.6 and 7.7 ppm are 0.2 and 0.1 ppm upfield shifted, respectively, with respect to H_β of the isonicotinate. Moreover, the peaks at 2.6 and 2.8 ppm corresponding to the NCH_3 and CH_2 protons of tmen appear as a doublet instead of a sharp singlet indicating the presence of both the square and the triangle as observed recently by Hollo-Sitkey et al. in a mixture of squares and triangles.[16n] This observation also indicates the formation of both symmetrical **2a** and **2b** in solution at room temperature.

Mass Spectrometry. Although the NMR study gives the primary indication of the self-assembly reaction, it does not give any information on the exact composition and the nature of the species (squares or triangles). Mass spectrometry is established to be a good tool to determine the species in the solution. ESI can be used as the soft ionization method in this case because of the weak coordinative bonds in supramolecular assemblies.[15] The supramolecular complexes can be ionized in the ESI ion source by stripping off some counteranions and generating species of different charges. Figure 4A shows the ESI mass spectrum of the equimolar reaction mixture of *cis*-(dppf)$Pd(OTf)_2$ and Na-isonicotinate after formation of the complexes in solution. The peak at $m/z = 1714.6$ corresponds to M^{2+} for the square **1a** which comes after removal of two triflate anions from the square and can be considered $[M_{1a} - 2CF_3SO_3^-]/2$; the peak at 1249.0 corresponds to M^{2+} for the triangle **1b**. Similarly, the peak at 782.00 corresponds to the M^{4+} of the square **1a** and M^{3+} of the triangle **1b** which may be considered as $[M_{1a} - 4CF_3SO_3^-]/4$ for the square and $[M_{1b} - 3CF_3SO_3^-]/3$ for the triangle. The intensity of the peak for M^{2+} of the square **1a** is less than that of the triangle **1b**. Figure 4B shows the ESI mass spectrum of **2a**−**2b** in methanolic solution. The peak at 752.20 is due to the M^{2+} of the square **2a** which comes after removal of two nitrate anions from the square **2a** and can be considered as $[M_{2a} - 2NO_3^-]/2$ and a small peak at 547.00 appears which corresponds to M^{2+} of the triangle **2b**. The most intense peak at 344.5 corresponds to M^{4+} of the square and M^{3+} of the triangle which can be represented as $[M_{2a} - 4NO_3^-]/4$ for **2a** and $[M_{2b} - 3NO_3^-]/3$ for **2b**. So, mass spectrometry showed the formation of a mixture of squares and triangles in solution.

DOSY NMR Spectroscopy. To detect the simultaneous existence of squares and triangles in solution, a pulsed field gradient spin−echo NMR (PGSE) experiment was performed. The size of the supramolecules can be determined experimentally by measuring the diffusion coefficients.[16] In this case a rough approximation of each molecule can be considered as a sphere, and the radius of the sphere can be correlated to the diffusion coefficient according to Stokes−Einstein equation (eq 1).

$$D = k_B T/(6\pi\eta r) \quad (1)$$

where T is the absolute temperature, k_B the Boltzmann constant, r the hydrodynamic radius, and η the solvent viscosity at temperature T. The ^{1}H DOSY NMR study of both **1a**−**1b** and **2a**−**2b** will be discussed here.

The 2D DOSY NMR spectrum of **1a**−**1b** in methanol-d_4 is showed in Supporting Information. In the ^{1}H NMR spectrum two sets of signals appear for square **1a** and triangle **1b** for pyridine-H_α and pyridine-H_β protons at 8.2, 6.8, and 8.1, 6.7 ppm, respectively. However, both the sets of signals appeared in the DOSY NMR spectrum with the same diffusion coefficients. This can be attributed to the fast ligand exchange in the DOSY time scale in methanol-d_4 for **1a** and **1b** (Figure S3, Supporting Information). The fast ligand exchange in case of **1a**−**1b** compared to **2a**−**2b** may be due to the presence of π acceptor dppf ligand in case of **1a**−**1b**. As the π acceptor dppf ligand has larger trans-effect compared to the N-donor tmen ligand, the exchange rate of isonicotinate ligands trans to dppf in **1a**−**1b** are faster than the exchange rate of the same ligands trans to tmen in **2a**−**2b**. As the ^{1}H NMR spectrum of this system was too complex, we used ^{31}P NMR as a tool to assign the peaks due to **1a** and **1b**. In principle, the assignment of the peaks due to the square and triangle should be strongly supported by the effect of concentration on the equilibrium. The

(16) (a) Kapur, G. S.; Findeisen, M.; Berger, S. *Fuel* **2000**, *79*, 1347. (b) Consoli, G. M. L.; Granata, G.; Garozzo, D.; Mecca, T.; Geraci, C. *Tetrahedron Lett.* **2007**, *48*, 7974. (c) Cabrita, E. J.; Berger, S.; Brauer, P.; Karger, J. *J. Magn. Reson.* **2002**, *157*, 124. (d) Eads, C. D.; Noda, I. *J. Am. Chem. Soc.* **2002**, *124*, 1111. (e) Delsuc, M. A.; Malliavin, T. E. *Anal. Chem.* **1998**, *70*, 2146. (f) Durand, E.; Clemancey, M.; Quoineaud, A.-A.; Verstraete, J.; Espinat, D.; Lancelin, J.-M. *Energy Fuels* **2008**, *22*, 2604. (g) Nilsson, M.; Morris, G. A. *Anal. Chem.* **2008**, *80*, 3777. (h) Antalek, B. *Concepts Magn. Reson., Part A* **2007**, *30*, 219. (i) Lucas, L. H.; Otto, W. H.; Larive, C. K. *J. Magn. Reson.* **2002**, *156*, 138. (j) Kapur, G. S.; Cabrita, E. J.; Berger, S. *Tetrahedron Lett.* **2000**, *41*, 7181. (k) Macchioni, A.; Ciancaleoni, G.; Zuccaccia, C.; Zuccaccia, D. *Chem. Soc. Rev.* **2008**, *37*, 479. (l) Pastor, A.; Martinez-Viviente, E. *Coord. Chem. Rev.* **2008**, *252*, 2314. (m) Ferrer, M.; Gutierrez, A.; Mounir, M.; Rossell, O.; Ruiz, E.; Rang, A.; Engeser, M. *Inorg. Chem.* **2007**, *46*, 3395. (n) Hollo-Sitkey, E.; Tarkanyi, G.; Parkanyi, L.; Megyes, T.; Besenyei, G. *Eur. J. Inorg. Chem.* **2008**, 1573.

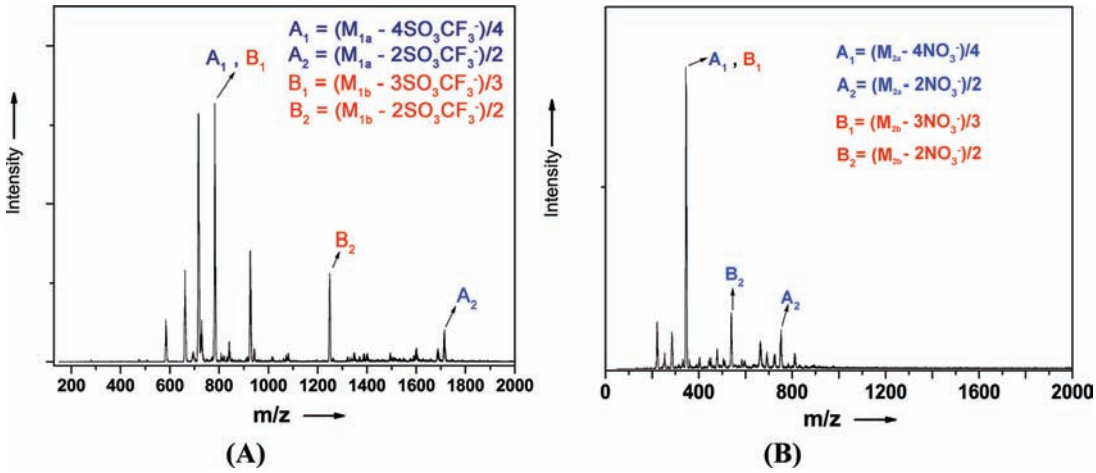

Figure 4. Mass spectra of **1a**−**1b** (A) and **2a**−**2b** (B) in methanol.

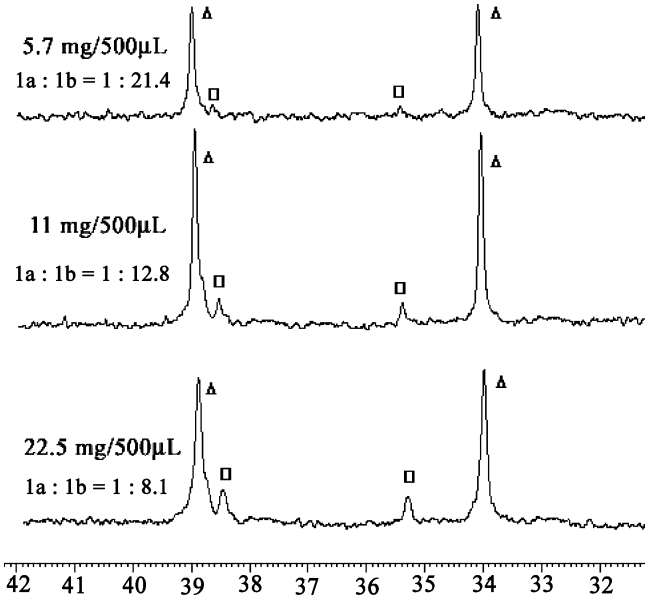

Figure 5. $^{31}P\{^1H\}$ NMR spectra of **1a/1b** at different concentrations in methanol-d_4.

equilibrium between the triangle and square can be written as

$$4\triangle \overset{K}{\rightleftharpoons} 3\square \qquad \text{where} \qquad K = \text{equilibrium constant}$$

As per the Le Chatelier's principle, with increase in concentration of the components in the mixture the equilibrium will shift from triangle to square. With increase in the concentration of the **1a**−**1b** mixture, the intensity ^{31}P NMR peak of the minor product increases gradually (Figure 5). This observation is in strong support that indeed the minor product in the solution is square.

The signals for the Py-H_α and Py-H_β protons in ^1H NMR spectra of **2a**−**2b** were well separated in the case of square **2a** and triangle **2b**. Hence, in the case of ^1H DOSY NMR spectra the peaks at 8.9 ppm, 8.8 ppm, 7.7 ppm, and 7.6 ppm were taken into account, and the diffusion coefficients for these peaks have been measured from the plot of gradient strength vs the log of difference of intensity (Table 1). For **2a**−**2b** two different diffusion coefficients in methanol-d_4

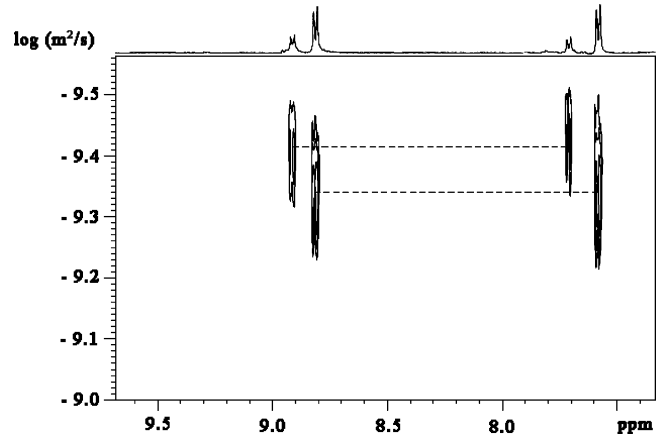

Figure 6. 2D ^1H DOSY NMR spectra of **2a/2b** recorded at 273 K in methanol-d_4.

Table 1. Peaks and the Corresponding Diffusion Coefficients of **2a/2b**

peak (ppm)	diffusion coefficient × 10^{-10} (m^2/s)
8.9	4.032
8.8	4.588
7.7	3.962
7.6	4.59

are clearly observed in Figure 6. This indicates that the ligand exchange between **2a**−**2b** is slow in the DOSY NMR time scale under this condition.

The diffusion coefficients for the peaks at 8.9 ppm and 7.7 ppm are smaller than those for the peaks at 8.8 ppm and 7.6 ppm. Hence, the peaks at 8.9 ppm and 7.7 ppm can be correlated to the square **2a** and the peaks at 8.8 ppm and 7.6 ppm can be correlated to the triangle **2b**. From Table 1 the ratio of the diffusion coefficients of the peaks at 8.9 ppm and 8.8 ppm as well as at 7.7 ppm and 7.6 ppm was found to be approximately 0.8, and the ratio of the hydrodynamic radius of the triangle **2b** to the square **2a** is also 0.8. A similar ratio between hydrodynamic radius of square and triangle has been recently reported for other triangle/square equilibria.[16m,n] Hence the result of the ^1H DOSY NMR (Figure 6) clearly suggests that at room temperature in solution triangle **2b** (more intense peaks at 8.8 ppm and 7.6 ppm in ^1H NMR spectra) remains as the major component with respect to the square **2a** (less intense peaks at 8.9 ppm and 7.7 ppm in ^1H NMR spectra).

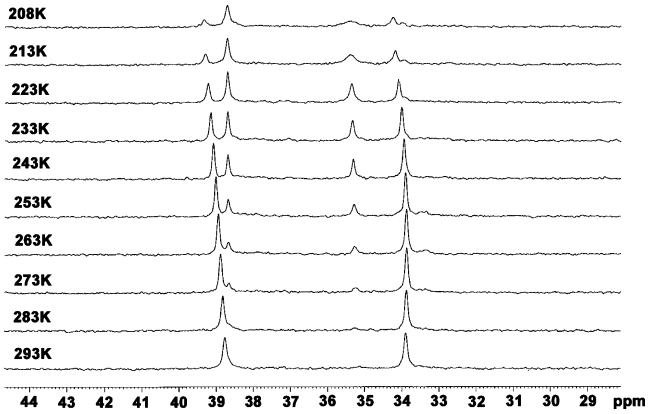

Figure 7. Variable temperature ^{31}P NMR of **1a** and **1b** in methanol.

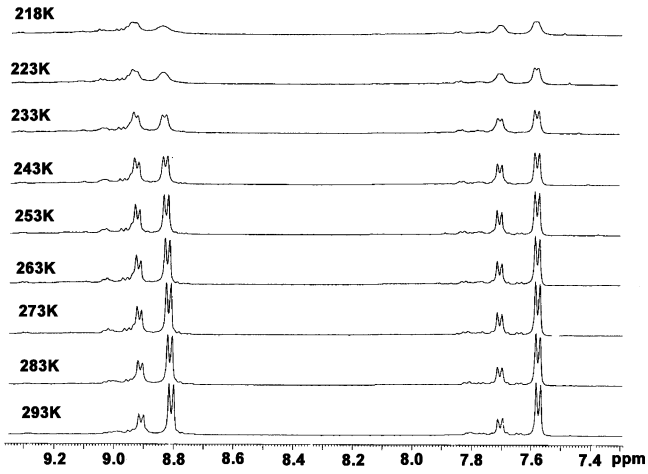

Figure 8. Variable temperature ^{1}H NMR spectra of **2a**−**2b** in methanol.

Temperature Effects on the Equilibrium. The equilibrium between **1a** vs **1b** and **2a** vs **2b** can be significantly influenced by temperature. The ^{31}P NMR spectra of the mixture of **1a** and **1b** in methanol-d_4 were recorded at temperatures varying from 293 to 208 K in 10 K intervals. At 293 K only two sharp peaks come at 38.8 ppm and 33.9 ppm (Figure 7), whereas at 273 K two small peaks arise at 38.7 ppm and 35.3 ppm and with further lowering of temperature the intensity of these peaks increases. As the diffusion correlation NMR suggests the intensity of the peaks at 38.8 ppm and 33.9 ppm, which may be considered for the triangle **1b**, decreases whereas the intensity of the peaks at 38.7 ppm and 35.3 ppm considered for square **1a** increases with lowering of temperature.

At 233 K the intensity of the peaks corresponding to the square **1a** and the triangle **1b** becomes almost equal. In the case of **2a** and **2b** the proton NMR spectra were recorded at temperatures varying from 293 to 218 K by an interval of 10 K. The intensity of the peaks at 8.9 ppm and 7.7 ppm which are due to the square **2a** (as the DOSY NMR suggests) increase by lowering of temperature whereas the intensity of the peaks at 8.8 ppm and 7.6 ppm which are corresponding to the triangle **2b** decreases.

At 243 K the intensity of the peaks for both square **2a** and triangle **2b** becomes equal (Figure 8). Equilibrium constants for the square-triangle equilibria (for **1a**−**1b** and **2a**−**2b**) can be determined from eqs 2 and 3.

$$K = \frac{[\text{triangle}]^4}{[\text{square}]^3} \tag{2}$$

$$\ln k = -\frac{\Delta G_{eq}}{RT} = -\frac{\Delta H_{eq}}{RT} + \frac{\Delta S_{eq}}{R} \tag{3}$$

The values of ΔH_{eq} and ΔS_{eq} can be determined from the plots of ln K against $1/T$ according to eq 3 (Supporting Information, Figure S1 and Figure S2). The values of ΔH_{eq} and ΔS_{eq} for the **1a**−**1b** and **2a**−**2b** square−triangle equilibria were calculated from the respective plots of ln K versus $1/T$ and were found to be 17.43 ± 1.27 kJ mol^{-1} and 81.20 ± 5.10 J mol^{-1} K^{-1} for **2a**−**2b** and 53.70 ± 2.30 kJ mol^{-1} and 236.1 ± 9.97 J mol^{-1} K^{-1} for **1a**−**1b**, respectively. The large positive value of ΔH in both the cases indicates the greater strain in the molecular triangles **1b** and **2b** compared to the corresponding squares **1a** and **2a**. The greater value of ΔH_{eq} (53.70 kJ mol^{-1}) in the case of **1a**−**1b** compared to that of **2a**−**2b** (17.43 kJ mol^{-1}) can be accounted for the larger strain in **1a**−**1b** as a result of the presence of large ferrocenyl moieties and phenyl rings in the corner of **1a**−**1b** rather than small tmen moieties in the corner of **2a**−**2b**. The positive entropy in both **1a**−**1b** and **2a**−**2b** overcomes the positive enthalpy at higher temperature by the term $-T\Delta S_{eq}$. Increase in the amount of square upon cooling can be explained by the thermodynamic parameters. The positive ΔH value for the **1a**−**1b** equilibrium indicates that the formation of triangle **1b** from the corresponding square **1a** is an endothermic process. As per the Le Chatelier's principle, the reaction proceeds in the backward direction upon further cooling of the reaction medium, and thus more of the square will form.

Crystal Structures of 1a and 2a. Red color crystals of **1a** were grown from the wine red methanolic reaction mixture by slow diffusion of ether. Crystals become amorphous in a few seconds upon being taken out of the mother liquor. Structure determination confirmed the formation of the square **1a** (Figure 9), although an equilibrium exists between the square **1a** and the triangle **1b** in solution. Structure refinement parameters are assembled in Table 2, and the selected bond parameters are shown in Table 3.

The structure contains four triflate counteranions and three unique methanol molecules in the lattice per square molecule. The cationic square molecules are stacked to form one-dimensional square shaped channels containing methanol molecules (Figure 10[14]). Two methanol molecules are H-bonded to the carboxylate oxygens O(4) and O(2) in the square. The hydrogen bond distances are of O(81)−H(81)···O(4) = 2.900(4)Å and O(82)−H(82)···O(2) = 2.813(6) Å, respectively. Similarly the third methanol molecule was hydrogen bonded to the O(1A) of the $CF_3SO_3^-$ anion with a distance of O(83A)−H(83A)···O(1A) = 2.766(4) Å. The shortest Pd−Pd distance between the parallel squares in the solid state is 13.12 Å. The disordered triflate counteranions remain in between two square molecules.

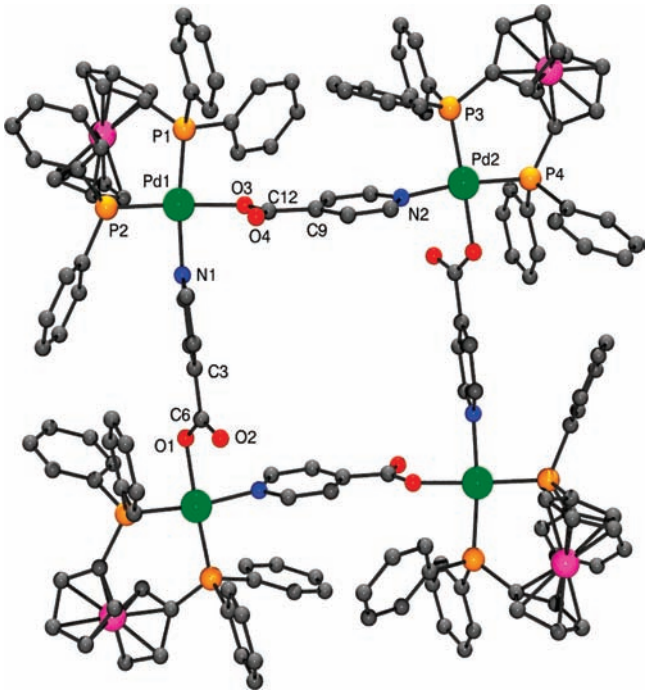

Figure 9. Molecular view of the square **1a** with atom numbering scheme. Anions and solvent molecules are omitted for the sake of clarity.

Table 2. Crystallographic Data and Details of Refinements for **1a** and **2a**

	1a	**2a**
empirical formula	$C_{170}H_{152}F_{12}Fe_4N_4O_{26}P_8Pd_4S_4$	$C_{48}H_{80}Cl_4N_{12}O_{24}Pd_4$
fw	3919.961	1776.64
crystal system	triclinic,	tetragonal
space group	$P\bar{1}$	$I\bar{4}$
a, Å	13.1243(3)	20.8701(19)
b, Å	18.9229(4)	20.8701(19)
c, Å	20.2725(5)	9.6882(17)
α, deg	101.0170(10)	90
β, deg	105.5100(10)	90
γ, deg	105.5460 (10)	90
V, Å^3	4482.70(18)	4219.8(9)
Z	1	2
ρ_{calcd}, g cm^{-3}	1.452	1.398
μ, mm^{-1}	0.901	1.032
$F(000)$	1988	1792
θ range, deg	1.71−27.50	1.95−24.97
total data	20555	3721
temp, K	123	150
GOF[a]	1.059	1.196
R1[b] $[I > 2\sigma(I)]$	0.0374	0.1173
wR2[c] $[I > 2\sigma(I)]$	0.0882	0.3057

[a] GOF = $\{\sum[w(F_o^2 - F_c^2)^2]/(n-p)\}^{1/2}$, where n and p denote the number of data points and the number of parameters, respectively. [b] R1 = $(\sum||F_o| - |F_c||)/\sum|F_o|$. [c] wR2 = $\{\sum[w(F_o^2 - F_c^2)^2]/\sum|w|(F_o^2)^2]\}^{1/2}$, where $w = 1/[\sigma^2(F_o^2) + (aP)^2 + (bP)]$ and $P = [\max(0, F_o^2) + 2F_c^2]/3$.

Two of the three methanol molecules per square molecule run through the channel formed by the square molecules. The coordination geometry around the Pd(II) centers is pseudo-square planar with the P−Pd distance of ∼2.3 Å and the P−Pd−P bite angle of 95.93°. The N−Pd−O angle is 86.7°, and the N−Pd and O−Pd bond distances are 2.08 Å and 2.06 Å, respectively (Table 3). The intramolecular shortest Pd−Pd distance is 8.97 Å, which measures the length of the square. The triangular analogue was not crystallized, although both mass spectrometry and NMR suggest that the triangle **1b** remains as the major component with respect to

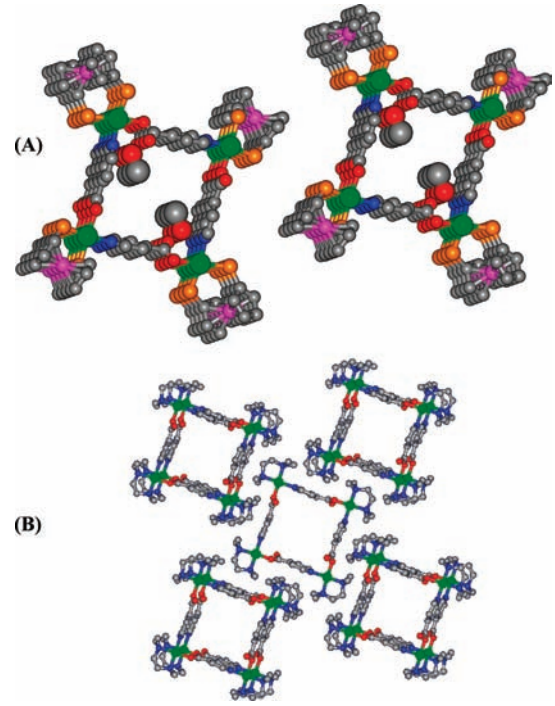

Figure 10. (A) Packing view of the square **1a** in solid state showing the methanol molecules in the channel. Phenyl rings of the dppf ligands and the OTf counteranions are omitted for the sake of clarity. (B) Packing view of **2a** in solid sate, counteranions are omitted for clarity.

Table 3. Important Bond Lengths (Å) and Angles (deg) for Complexes **1a** and **2a**

		1a	
Pd(1)−N(1)	2.083(2)	Pd(1)−P(1)	2.3029(6)
Pd(1)−P(2)	2.2608(6)	Pd(1)−O(3)	2.0601(18)
Pd(2)−N(2)	2.086(2)	Pd(2)−P(3)	2.261(6)
Pd(2)−P(4)	2.277(6)	Pd(2)−O(1)	2.062(17)
O(1)−C(6)	1.279(3)	O(2)−C(6)	1.225(3)
O(3)−C(12)	1.281(3)	O(4)−C(12)	1.232(4)
O(3)−Pd(1)−N(1)	86.70(8)	O(3)−Pd(1)−P(2)	175.6(6)
N(1)−Pd(1)−P(2)	91.10(6)	O(3)−Pd(1)−P(1)	85.85(5)
N(1)−Pd(1)−P(1)	170.5(6)	P(2)−Pd(1)−P(1)	95.93(2)
N(2)−Pd(2)−P(3)	88.73(6)	N(2)−Pd(2)−P(4)	170.6(6)
P(3)−Pd(2)−P(4)	99.82(2)		
		2a	
Pd(1)−O(1)	1.952(12)	Pd(1)−N(1)	2.031(12)
Pd(1)−N(2)	2.046(18)	Pd(1)−N(3)	2.066(10)
O(1)−C(12)	1.270(18)	O(2)−C(12)	1.261(17)
O(1)−Pd(1)−N(1)	90.6(5)	O(1)−Pd(1)−N(2)	170.7(14)
N(1)−Pd(1)−N(2)	86.1(6)	O(1)−Pd(1)−N(3)	90.2(5)
N(1)−Pd(1)−N(3)	177.3(9)	N(2)−Pd(1)−N(3)	92.8(6)

the square **1a** in the solution. This may be due to high lattice energy of formation of the square compared to the triangle in solid state at room temperature.

In the case of **2a,** two equivalents of tetraethyl ammonium perchlorate were added into the methanolic solution, and the cream-colored precipitate obtained was dissolved in nitromethane. Needle shaped pale yellow crystals were grown by slow diffusion of diethyl ether into the nitromethane solution over three days. Several attempts to crystallize the nitrate analogue of the square resulted in the formation of microcrystalline powder. One suitable single crystal was mounted under paratone oil, and the data were collected at 150 K. The structure showed the formation of the square **2a**

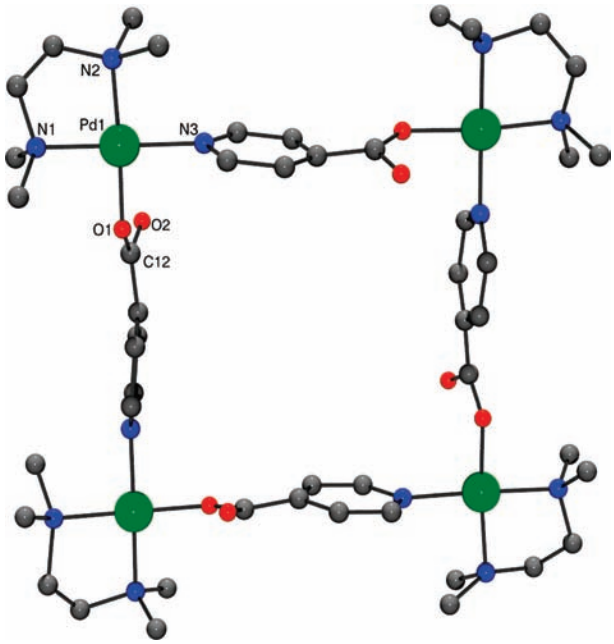

Figure 11. Molecular view of the square **2a** with atom numbering scheme. Counter anions and hydrogens are omitted for the sake of clarity.

although both the square **2a** and the triangle **2b** were in equilibrium in solution. As the square **2a** was crystallized from nitromethane solution, it was of our interest to see whether the nitromethane solution contains either both the components or the square alone. NMR in nitromethane-d_3 showed the presence of both square and triangle in solution (Supporting Information). All the four Pd(II) centers in the structure were identical with a PdN_3O coordination environment (Figure 11). Four highly disordered perchlorate counteranions were present in the lattice per molecule of the square. All the N−Pd bonds were ∼2 Å, the bite angle formed by the bidentate tmen is 86.24°, and the N−Pd−O angle is 89.10°. Hence, the environment around the palladium is almost square-planar. Packing in the solid state showed the stacking of one molecule over the other to form square shaped open frameworks containing no solvent or counteranions (Figure 10). The crystallographic information and structure refinement parameters for both **1a** and **2a** have been assembled in Table 2, and the CIF corresponding to the structures **1a** and **2a** have been given in Supporting Information.

Conclusion

Coordination driven self-assembly reactions of a nonsymmetric ambidentate ligand isonicotinate with two different *cis*-blocked square planar Pd(II) 90° acceptors resulted in the formation of dynamic equilibria between [4 + 4] and [3 + 3] assembled macrocycles. Although quite a few examples of square−-triangle equilibria have been reported in the literature, no such example is known using a nonsymmetrical linker because of the possibility of formation of a mixture of several linkage isomeric triangles and squares due to different connectivities of the nonsymmetrical linker (Supporting Information). Much to our surprise, only a mixture of symmetrical isomeric triangles and squares has been formed in both of the cases (**1a**−**1b** and **2a**−**2b**). The equal electron density distribution around the Pd(II) centers is probably a reason for the formation of these four symmetrical linkage isomers. The detailed thermodynamic and kinetic behavior of both the equilibria have been studied using NMR techniques. Though square was the species that crystallized predominantly in both cases, the solution composition was surprisingly a mixture of square and triangle with the latter one as the major component in both the cases. The ratio of the component depends on the temperature as well as the concentration of the medium. Temperature dependent NMR study in case of the **1a**−**1b** equilibrium showed the preference of formation of the entropy-favored triangle (**1b**) in solution. Decrease in temperature favored the formation of more molecular squares (**1a**). Similarly, an increase in concentration of the reaction mixture increases the amount of squares in the mixture, which was corroborated well with the Le Chatelier's principle. The exclusive formation of the squares in both the cases may be due to the high lattice energy of formation compared to the triangles.

Experimental Section

Materials and Methods. ^{1}H and ^{31}P NMR spectra were recorded on a Bruker Avance 400 (400 and 162 MHz, respectively) instrument with the solvent signals as the internal standard. ESI mass spectra were recorded on FINNIGAN LCQ DECAXP MAX mass spectrometer. Elemental analyses (C, H, N) were performed using a Perkin-Elmer 240-CHNS analyzer. Ionization parameters were adjusted as follows: capillary voltage 29.71 V and tube lens voltage −60.00 V. *cis*-(dppf)$PdCl_2$, *N*,*N*,*N*′,*N*′-tetramethyethane-1,2-diamine (tmen), isonicotinic acid, silver triflate (AgOTf), and deuterated solvents were purchased from Aldrich Chemical company and were used without further purification. *cis*-(dppf)$Pd(OTf)_2$[17] and *cis*-(tmen)$Pd(NO_3)_2$[18] were prepared according to the literature procedure treating the corresponding chlorides with two equivalents of appropriate silver salts followed by filtration of the AgCl precipitate through a celite bed.

Synthesis of 1a−**1b.** To a 2-mL methanol solution containing 10.8 mg (0.01 mmol) of *cis*-(dppf)$Pd(H_2O)_2(OTf)_2$, a methanol solution of 1.5 mg (1 mL) of Na-isonicotinate (0.01 mmol) was added drop-by-drop with continuous stirring (5 min). A sharp color change from light blue to wine red was noticed. Ether was added to the solution to obtain the product as red precipitate. **1a**: $C_{164}H_{128}F_{12}O_{20}N_4P_8S_4Fe_4Pd_4$, 3723.92 g/mol. **1b**: $C_{123}H_{96}F_9O_{15}N_3P_6S_3Fe_3Pd_3$, 2792.94 g/mol. ^{1}H NMR (methanol-d_4, 400 MHz, 273 K): 8.20 (**1a**), 8.10 (**1b**) (d, Py-H_α); 7.86−7.10 (m, phenyl); 6.90 (**1a**), 6.77 (**1b**) (d, Py-H_β); 5.20 (**1a**), 5.30 (**1b**) (d, Cp-H); 4.40 (**1a**), 4.47 (**1b**) (dd, 12H, Cp-H); 3.56 (**1a**), 3.77 (**1b**) (d, Cp-H) ppm. ^{31}P NMR (methanol-d_4, 162 MHz, 273 K): 38.7 and 35.3 (**1a**); 38.8 and 33.9 (**1b**) ppm. ESI-MS (methanol): m/z = 1714.60 $[M_{1a} - 2CF_3SO_3^-]^{2+}$; 1249.00 $[M_{1b} - 2CF_3SO_3^-]^{2+}$; 782.00 $[M_{1a} - 4CF_3SO_3^-]^{4+}$, $[M_{1b} - 3CF_3SO_3^-]^{3+}$. Anal. Calcd for $(C_{41}H_{32}NO_5P_2PdF_3SFe)_n$: C, 52.79; H, 3.43; N, 1.50%. Found: C, 52.48; H, 3.62; N, 1.72%. Isolated yield: 8.5 mg (91%).

Synthesis of 2a−**2b.** To a 3-mL methanol solution containing 3.5 mg (0.01 mmol) of *cis*-(tmen)$Pd(NO_3)_2$, a 2 mL methanol solution of 1.5 mg (1 mL) of Na-isonicotinate (0.01 mmol) was

(17) Stang, P. J.; Olenyuk, B.; Fan, J.; Arif, A. M. *Organometallics* **1996**, *15*, 904.
(18) Lim, M. C.; Martin, R. B. *J. Inorg. Nucl. Chem.* **1976**, *38*, 1911.

added drop-by-drop with continuous stirring (30 min). The yellow reaction mixture was concentrated to 1 mL and diethyl ether was added to obtain the product as yellow powder. The methanolic solution of the product was treated with slight excess of Et_4NClO_4 to obtain the perchlorate analogue of the product as a cream color precipitate. **2a** (nitrate analogue): $C_{48}H_{80}N_{16}O_{20}Pd_4$, 1624.18 g/mol. **2b**: $C_{36}H_{60}N_{12}O_{15}Pd_3$, 1218.14 g/mol. ^{1}H NMR (methanol-d_4, 400 MHz, rt): 8.90 (**2a**), 8.80 (**2b**) (d, Py-H_α); 7.70 (**2a**), 7.60 (**2b**) (d, Py-H_β); 2.80 (d, CH_2); 2.60 (d, CH_3) ppm. ESI-MS (methanol): m/z = 752.20 $[M_{2a} - 2NO_3^-]^{2+}$; 547.00 $[M_{2b} - 2NO_3^-]^{2+}$; 344.53 $[M_{2a} - 4NO_3^-]^{4+}$, $[M_{2b} - 3NO_3^-]^{3+}$. Anal. Calcd for $(C_{12}H_{20}N_4O_5Pd)_n$: C, 35.44; H, 4.96; N, 13.77%. Found: C, 35.68; H, 4.71; N, 13.62%. Isolated yield: 3.5 mg (86%).

Crystallography. Both the samples displayed rapid loss of solvent when removed from the mother liquor. X-ray data were collected using a Bruker X8 Apex II diffractometer equipped with monochromated Mo Kα radiation (λ = 0.71073 Å). Collection temperatures were maintained at 123 and 150 K for **1a** and **2a**, respectively. Data integration and scaling were performed using the Bruker Apex II suite of programs and corrected for the effects of absorption with SADABS.[19] Initial structure solutions were obtained via direct methods with SHELXS-97[20] before refinement using conventional alternating cycles of least-squares on F^2 with SHELXL-97[20] using the graphical interface package X-Seed.[21] In all cases non-hydrogen atoms were refined anisotropically. Hydrogen atoms were fixed in idealized positions and allowed to ride on the atoms to which they were attached. Hydrogen atom thermal parameters were tied to the atom to which they were attached. In the case of complex **1a** only three unique methanol molecules could be accurately located from the Fourier difference map, although there was evidence of other highly disordered solvent. The SQUEEZE routine of PLATON[22] was used to calculate the residual electron density in the structure (216 electrons in 652 Å^3), which calculates as 12 methanol molecules per unit cell (giving a total of 18 methanol molecules per cell). One trifluoromethanesulfonate ($CF_3SO_3^-$) counteranion is disordered over two positions with the occupancies freely refined against each other (68:32). Cell parameters of several crystals were identical in both of the cases, which indirectly indicated the formation of square in both the cases.

Acknowledgment. Financial support by the Council of Scientific and Industrial Research (CSIR) and the Department of Science and Technology (DST-SR/S1/IC-18/2008), Govt. of India, is gratefully acknowledged. The authors thank Prof. Stuart R. Batten for his kind help on the X-ray structure determination of complex **1a**.

Supporting Information Available: X-ray crystallographic files for **1a** and **2a** in CIF format. ^{1}H NMR spectra of **2a**−**2b** mixture in nitromethane-d_3 and Vant-Hoff plots for the equilibrium of **1a**−**1b** and **2a**−**2b**, respectively, in PDF format. This material is available free of charge via the Internet at http://pubs.acs.org.

IC802254F

(19) *Apex II & SADABS*; Bruker AXS Ltd.: Madison, WI, 2005.
(20) Sheldrik, G. M. *SHELXS-97 & SHELXL-97*; University of Göttingen: Göttingen, 1997.
(21) Barbour, L. J. *J. Supramol. Chem.* **2001**, *1*, 189.
(22) Spek, A. L. *PLATON*; Utrecht University: Utrecht, 2002.